ISSN: 2229-7359 Vol. 11 No. 3S, 2025

https://www.theaspd.com/ijes.php

Synergistic Effects Of Polypyrrole-Doped Iron Oxide Nanoparticles: Unveiling Dual Roles In Antimicrobial Action And Accelerated Wound Healing

Arsha A¹ and Jeena Pearl A^{*}

¹Research Scholar, Department of Chemistry and Research centre, Scott Christian College (Autonomous) Nagercoil- 629003, Tamil Nadu, India.

(Affiliated to Manonmaniam Sundaranar University, Abishekapatti, Tirunelveli-627012, Tamil Nadu, India)

*Research Supervisor, Department of Chemistry and Research centre, Scott Christian College (Autonomous) Nagercoil- 629003, Tamil Nadu, India.

(Affiliated to Manonmaniam Sundaranar University, Abishekapatti, Tirunelveli-627012, Tamil Nadu, India)

E-mail ID: hentryarsha@gmail.com¹, jeenapearl@rediffmail.com*

:

ABSTRACT

Metal oxide-based nanomaterials are a substantial category of materials that are of great significance in both technological applications and scientific research. The purpose of this chapter is to present an overview of contemporary research into the production, characteristics, and applications of polymer/metal-oxide nanocomposites. The extract of *Amaranthus tricolor.L* was used to synthesise the Iron oxide nanoparticles, which were subsequently polymerised with pyrrole to produce iron oxide-doped polypyrrole. The produced nanocomposites were characterised using Fourier transform infrared spectroscopy (FT-IR), scanning electron microscopy (SEM), X-ray diffraction (XRD), and transmission electron microscopy (TEM). In addition to their beneficial effects in wound care and healing, the produced biocomposites exhibit robust antibacterial activity.

Keywords: Iron oxide, Nanocomposites, Amaranthus tricolor.L, Polypyrrole, Wound care

INTRODUCTION

Metal nanoparticles are of considerable interest owing to their wide-ranging applications in electronics, optoelectronics, antibacterial functions, and various medical fields such as treatment, diagnostics, and drug delivery [1–3]. The synthesis of metal nanoparticles has been achieved through various processes, encompassing chemical, physical, and environmentally friendly methods. Environmental pollution presents a significant issue due to the utilisation of chemical agents in the chemical approach, resulting in the production of substantial quantities of chemical waste as a byproduct. Nanoparticles are generated through several physical methods, such as spark discharge, pulsed laser ablation, and gamma irradiation.

Although these approaches are effective, they need a large quantity of pricey equipment. The manufacture of different metal nanoparticles is often performed using ecologically friendly approaches that include the use of plant extracts, bacteria, and fungus [4,5]. These technologies are ecologically sustainable, as proven by their shorter production timetables and lower prices when compared to other approaches. Metal nanoparticle manufacturing from plant chemicals is thought to be a simpler process than fungal or bacterial cultures, which require specialised skills and sterile settings to preserve. Furthermore, the plant extracts used to synthesise nanoparticles vary in size and form [6].

ISSN: 2229-7359 Vol. 11 No. 3S, 2025

https://www.theaspd.com/ijes.php

The synthesis of iron oxide (FeO) nanoparticles using plant materials provides numerous advantages in terms of ecofriendliness and compatibility for a variety of applications, as it does not require the use of hazardous compounds for the synthesis process [7]. Amaranthus tricolour L. is a green vegetable that is extensively cultivated in temperate and tropical regions and is similar to spinach, broccoli, and cabbage.. It is primarily ingested as a foliage vegetable and is commonly referred to as amaranth [8].

Due to their improved qualities over pure conducting polymers or inorganic materials, conducting polymer/inorganic composites are considered new materials[9]. Composites, known as "nanocomposites," have garnered attention recently. These materials cross the gap between conducting polymers and nanoparticles, making them important[10]. Polypyrrole is popular due to its distinctive electrical conductivity, redox characteristic, environmental stability, and ease of chemical and electrochemical synthesis [11].

2. MATERIALS AND METHODS

2.1 Materials

Amaranthus tricolor.L, Sodium Lauryl Sulfate, Pyrrole, Ethanol, Distilled water, Iron(III)chloridehexahydrate(FeCl₃.6H₂O), Buffer(CH₃COONa-CH₃COOH).

2.2 Biosynthesis of FeO nanoparticle

The leaves of Amaranthus tricolour. L were washed extensively with distilled water, then boiled for about 10 minutes. Then, the liquid was filtered using Whatman filter paper No. 1. A mixture of 20 ml of leaf extract and 0.1 g of FeCl₃.6H₂O was prepared by adding a buffer to get the pH level to 5.5. Centrifugation at 5000 rpm follows magnetic stirring for about 5 hours, during which the colour changes to dark brown. Then it's dried in a hot air oven after being rinsed with ethanol and distilled water.

2.3 Synthesis of Polypyrrole with FeO nanoparticle

One gramme of FeO nanoparticles was mixed with five grammes of Sodium Lauryl Sulphate in thirty millilitres of distilled water and subjected to ultrasonication for a duration of fifteen minutes. 0.1M of pyrrole was added to the previously mentioned solution and was subjected to ultrasonication for approximately 30 minutes. Combine 2.7 g of FeCl3.6H2O and stir for approximately 7 hours, then allow it to sit at room temperature for 24 hours. It was then filtered with ethanol and distilled water, followed by drying at room temperature.

2.4 Invitro wound healing assay

A scratch wound healing experiment was conducted utilising human dermal fibroblast (HDF) cells to assess the efficacy of FeO doped PolyPyrrole ($50 \mu g/ml$) in wound healing. The cells were cultivated in DMEM supplemented with 10% foetal bovine serum (FBS), 1% antibiotic-antimycotic solution, and high glucose. They were subsequently maintained in a humidified incubator at 37°C with 5% CO₂. The study employed cells at passage 15, with subculturing performed bi-daily. A monolayer exhibiting 80-100% confluence was established by seeding HDF cells in 12-well plates at a density of 0.25 million cells per well, followed by a 24-hour incubation period. Upon achieving confluence, a cross-shaped mark was created in each well utilising a sterile 200 μ L pipette tip. The pipette tip was maintained perpendicular to the well bottom to ensure a uniform scratch width. Following the careful removal of detached cells through two rinses with DMEM, the remaining adherent cells were treated with FPP at a concentration of 50 μ g/ml. The control wells included untreated cells and a standard control group administered 50 μ g/ml of povidone iodine. The plates were incubated for 48 hours at 37°C with 5% CO₂ to promote wound healing.Images of the scratch wound were taken at 0, 24, and 48 hours using an inverted

ISSN: 2229-7359 Vol. 11 No. 3S, 2025

https://www.theaspd.com/ijes.php

biological microscope (Olympus CKX415F, Japan), with the magnification settings kept constant. The degree of wound closure was quantified using ImageJ software, and the percentage of wound healing was calculated using the method below:

% of Wound Healing Scored = (Initial Area - Final Area) / Initial Area * 100 The experiment was duplicated three times, and the findings were reported as mean ± SD.

3. RESULT AND DISCUSSION

3.1 UV-Visible spectroscopy

The UV-Vis absorption peak at 411 nm for FeO-Polypyrrole might be attributed to the π - π * transitions of charge-transfer interactions between the FeO nanoparticles and the polypyrrole matrix. The existence of this value suggests that there is strong contact and doping between FeO and polypyrrole, which may improve the optical and electrical properties.

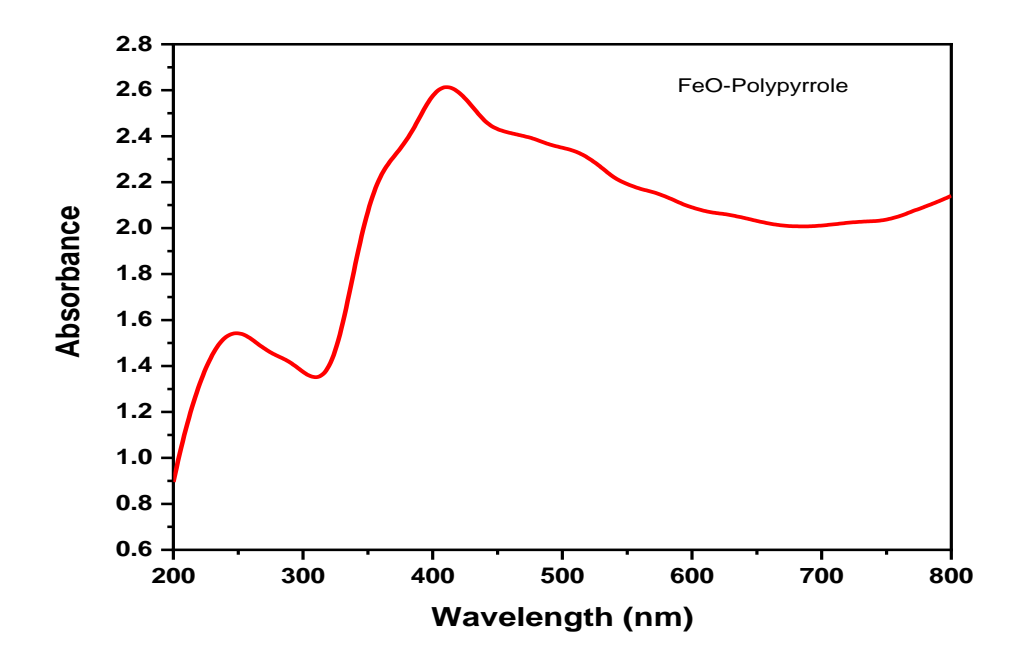


Fig 1. UV-Vis Spectroscopy of Feo doped Polypyrrole

3.2 FT-IR Spectroscopy

FT-IR spectroscopy of FeO-doped polypyrrole reveals interactions between structural and functional groups within the material, shown as characteristic absorption peaks. Matching O-H stretching allows the broad signal at 3435 cm⁻¹ to indicate the presence of adsorbed moisture or hydroxyl groups. C-H stretching vibrations of peaks at 2914 cm⁻¹. Characteristic of the polypyrrole backbone, the notable peak at 1637 cm⁻¹ is related with C=C stretching. Inside the polymer, C-N stretching or C-H bending vibrations produce the peaks at 1386 cm⁻¹ and 1455 cm⁻¹. The bands at 854 and 670 cm⁻¹ clearly indicate Fe-O vibrations, therefore confirming the presence of FeO nanoparticles in the polymer matrix. These findings support the structural integrity of the material and the efficient FeO doping of polypyrrole.

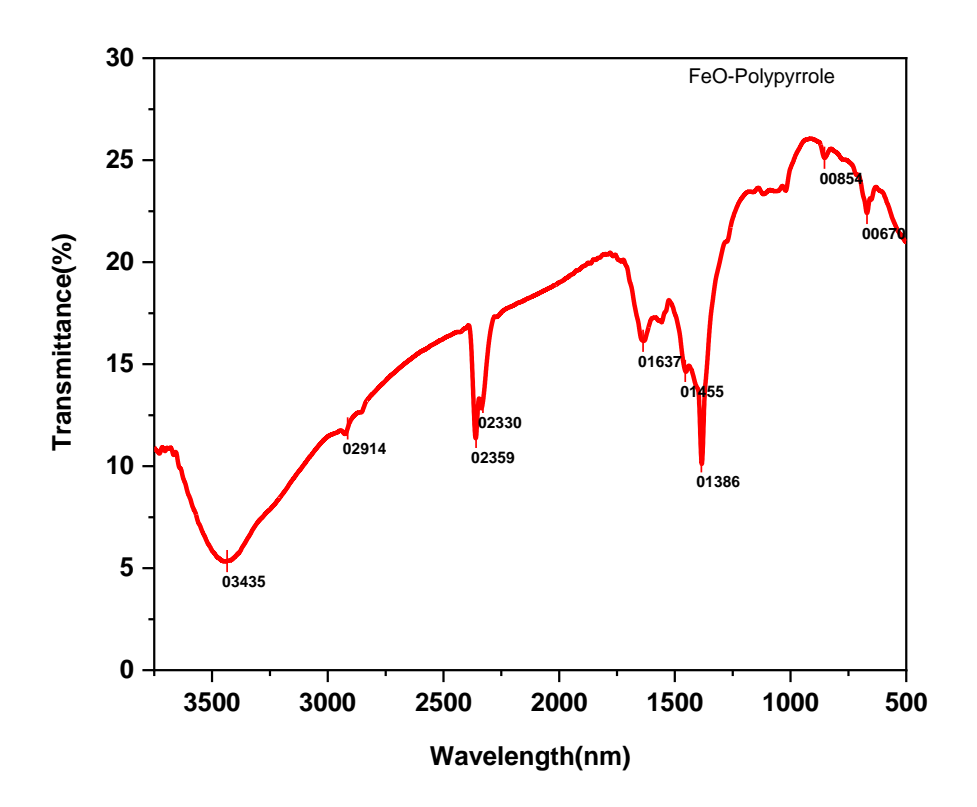


Fig 2. FT-IR Spectroscopy of FeO doped Polypyrrole

3.3 Scanning Electron Microscope (SEM)

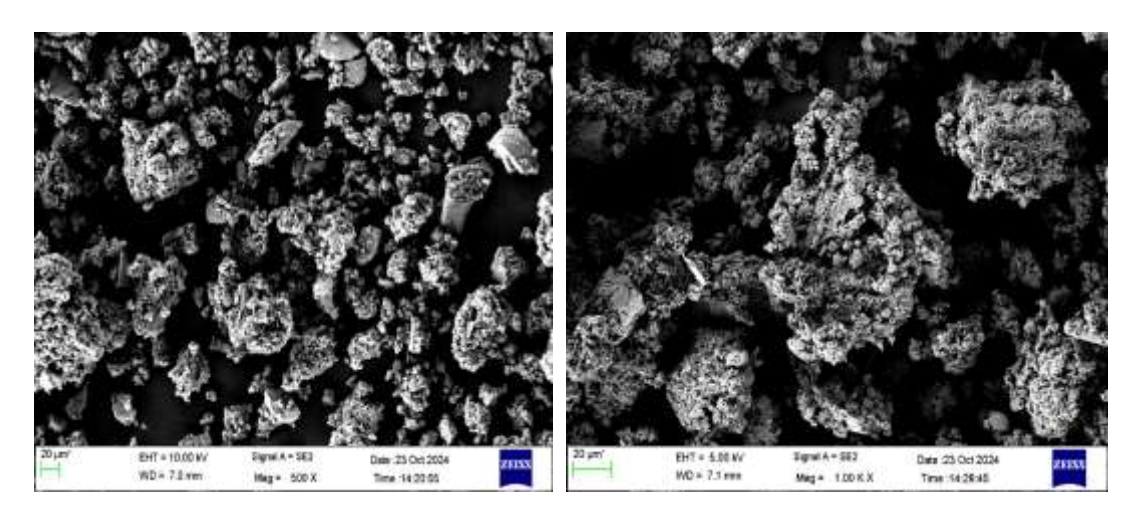


Fig 3. SEM image of FeO doped Polypyrrole

FeO-doped polypyrrole typically exhibits spherical particle formation with asymmetrical distribution. The observed morphology is due to the aggregation of FeO nanoparticles and their interactions with the polypyrrole matrix during the polymerization process. The synthesis process, reaction conditions, and FeO dispersion all have an impact on the final structure. The uneven distribution of FeO particles causes differences in particle size and shape.

3.4 Energy Dispersive X-ray Analysis (EDAX)

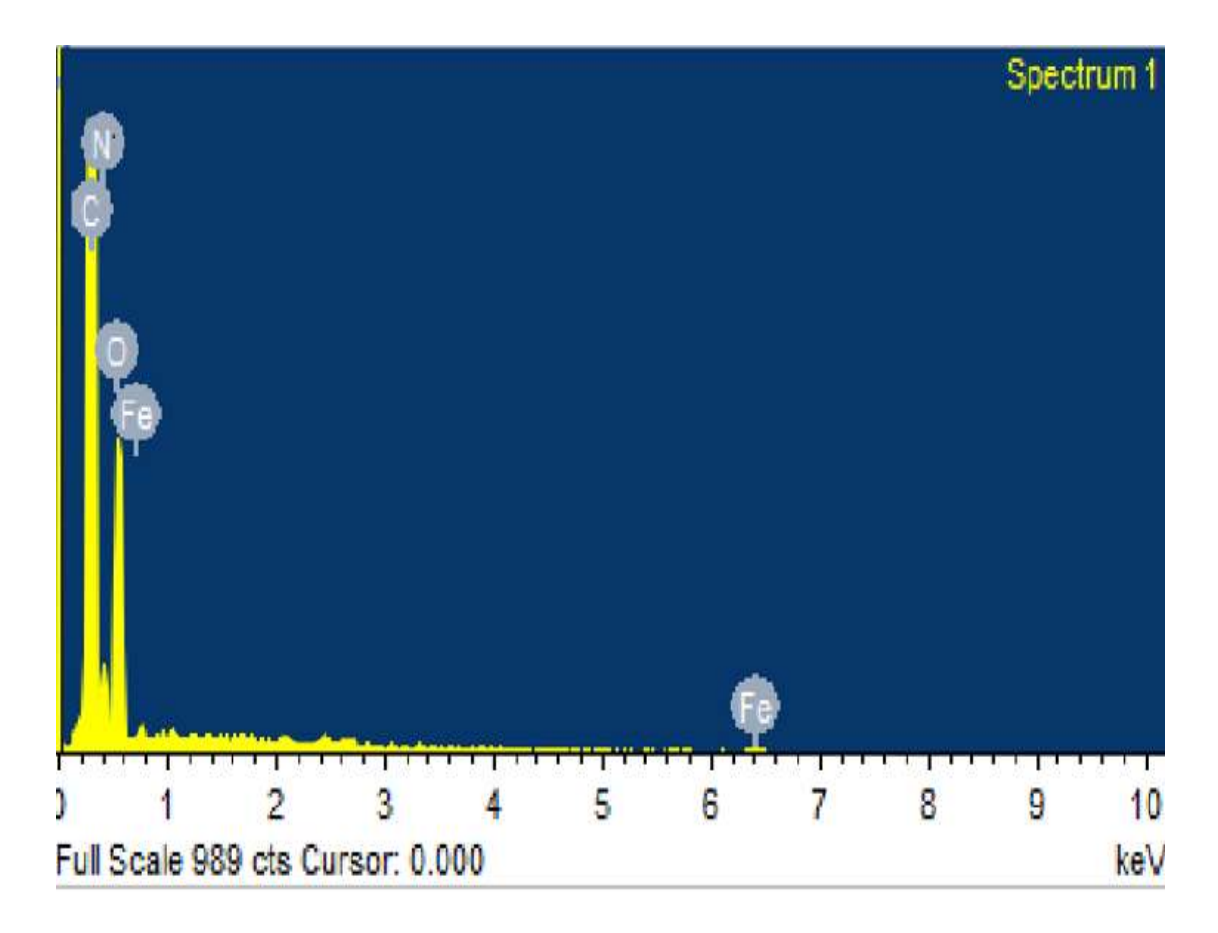


Fig 4. EDAX of Feo doped Polypyrrole

The EDAX spectrum of FeO-doped polypyrrole shows carbon (C), oxygen (O), nitrogen (N), and iron (Fe), as predicted. Oxygen comes mostly from the FeO nanoparticles and could also be present depending on oxidized species or adsorbed air oxygen inside the material. The polypyrrole structure is naturally nitrogenous as nitrogen is present in its pyrrole rings. Iron guarantees the effective doping of polypyrrole with FeO. These findings represent the incorporation of FeO into the polymer matrix and fit rather well with the desired material composition. Fig 4. shows the spectrum provides evidence that the sample contain Iron(Fe), Oxygen(O), Carbon(C) and Nitrogen(N). The peak energies are 0.2KeV, 0.3KeV, 0.4KeV and 6.4KeV.

3.5 X-Ray Diffraction Analysis(XRD)

The XRD pattern of FeO-doped polypyrrole exhibits broad peaks, indicating a predominantly amorphous nature with potential nanocrystalline domains. FeO crystallinity inside the polymer matrix is confirmed by the X-ray diffraction (XRD) pattern of FeO-doped polypyrrole (PPy), which exhibits peaks at coordinates of 33.1° and 36.1° (20). The amorphous character of Polypyrrole is shown by the significant hump that occurs and 40 degrees.

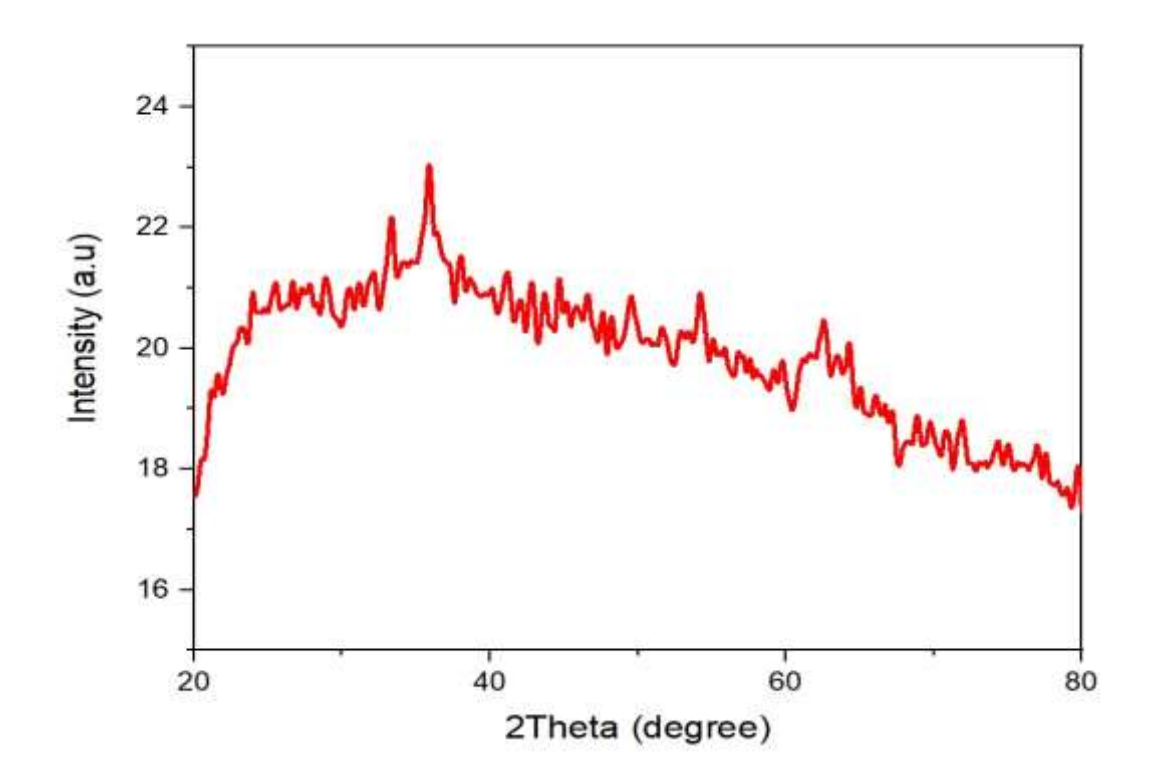


Fig 5. XRD of FeO doped Polypyrrole

4. APPLICATION

4.1 Wound healing on FeO doped polypyrrole

FPP (50 μg/ml) was tested in an in vitro scratch wound healing experiment on human dermal fibroblast (HDF) cells for 48 hours. After 48 hours, the untreated control group had 61% wound healing, demonstrating fibroblast cell migration and proliferation. In 48 hours, cells treated with 50 μg/ml FPP showed a considerable increase in wound closure, reaching 95-100%, indicating a strong pro-migratory and proliferative effect. Normal control (Povidone Iodine, 50 μg/ml) enhanced wound healing but had a lower closure rate than FPP. The gradual improvement in wound closure shows that FPP aids fibroblast migration and proliferation. FPP may aid early wound healing by encouraging cellular mobility and extracellular matrix remodelling due to its fast closure rate in the first 24 hours. It stimulates fibroblast activity as seen by its practically full recovery after 48 hours. Fibroblasts produce extracellular matrix proteins and growth factors needed for tissue regeneration, which aids angiogenesis and skin healing. FPP may increase new blood vessel formation, making it effective for skin repair therapy. This is backed by FPP-treated cells' improved wound healing. These findings imply that FPP and HDF cells may improve wound healing.

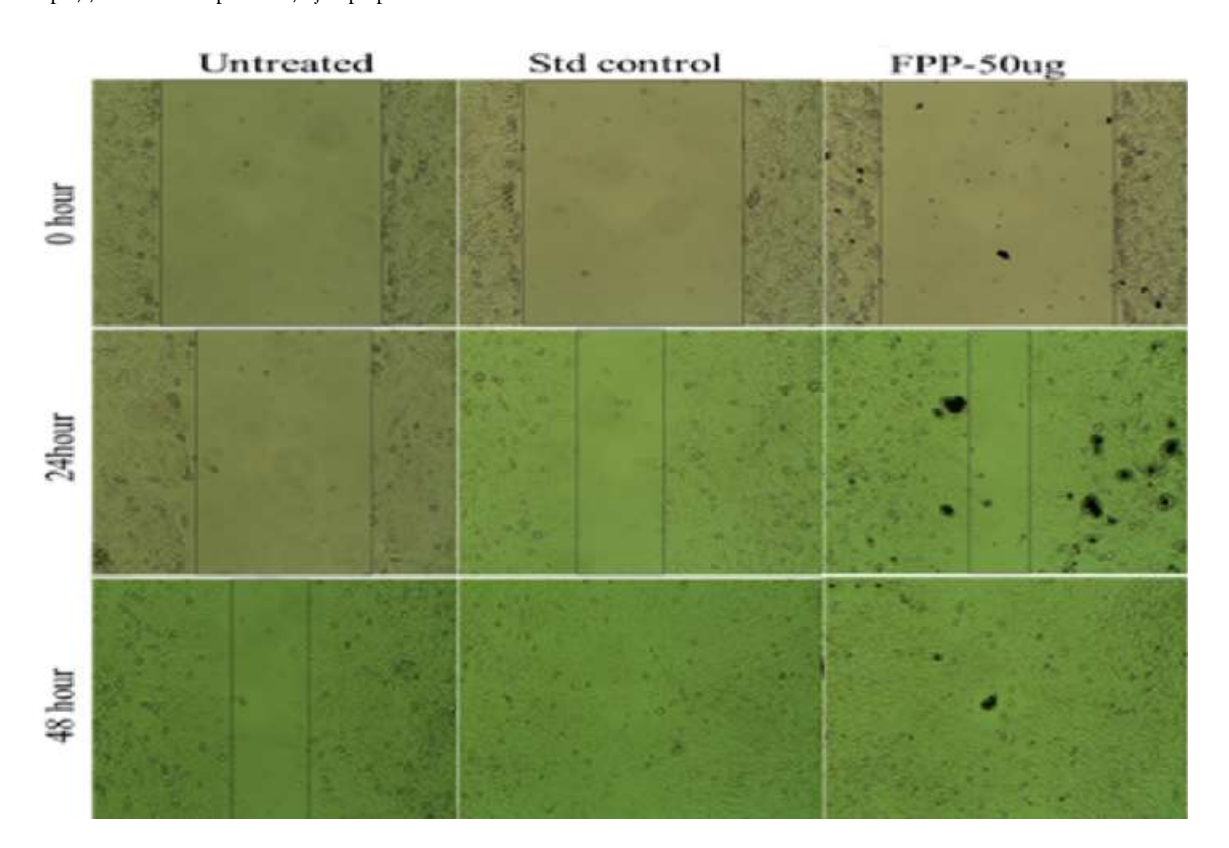


Fig 6. Wound healing of FeO-Polypyrrole

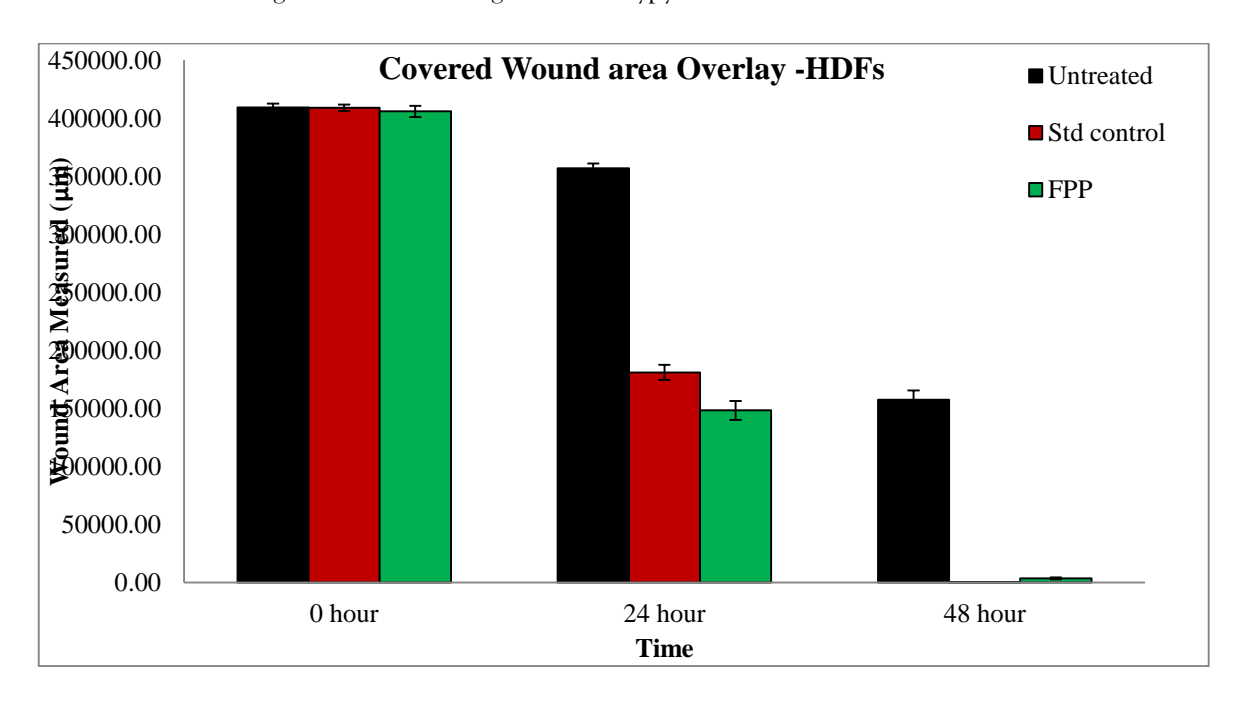


Fig 7. Wound healing graph of FeO-Polypyrrole

4.2 Antibacterial activity of FeO doped polypyrrole

FeO-doped polypyrrole demonstrated increased efficacy against Pseudomonas aeruginosa, exhibiting an inhibition zone of 17.5 mm compared to 14 mm in the control. Conversely, it displayed decreased activity against Streptococcus pneumoniae, with an inhibition zone of 16 mm compared to 19 mm in

ISSN: 2229-7359 Vol. 11 No. 3S, 2025

https://www.theaspd.com/ijes.php

the control. The enhanced effect on Pseudomonas aeruginosa may result from reactive oxygen species generation or membrane disruption, whereas the diminished effect on Streptococcus pneumoniae may be attributed to its thicker peptidoglycan layer, which limits FeO interaction.

Positive bacteria -->





doped

Negative bacteria->

Fig 8. Antibacterial activity of FeO

Polypyrrole

Bacteria	FeO- Polypyrrole	Control (Amikacin)
Pseudomonas aeruginosa	16mm	19mm
Streptococcus pneumoniae	17.5mm	14mm

Table 1. Antibacterial activity of FeO doped Polypyrrole

ISSN: 2229-7359 Vol. 11 No. 3S, 2025

https://www.theaspd.com/ijes.php

4.3 Antifungal activity of FeO doped polypyrrole

FeO-doped polypyrrole shown increased antifungal activity against Candida albicans and Aspergillus niger, with inhibition zones of 16.5 mm and 18 mm, respectively, compared to the 15 mm control. The enhanced suppression points to enhanced antifungal effectiveness, which may be brought on by the production of ROS, membrane rupture, or interference with the integrity of the fungal cell wall.

Fungi	FeO-Polypyrrole nanoparticle	Control (Nystatin)
Candida albicans	16.5mm	15mm
Aspergillus niger	18mm	15mm

Table 2. Antifungal activity of FeO doped Polypyrrole





Fig 9. Antifungal activity of FeO doped Polypyrrole

5. CONCLUSION

The characterisation of FeO-doped polypyrrole (FPP) confirms its successful synthesis and its applications in medicine. An absorption peak at 411 nm in UV-Vis spectroscopy indicates that effective FeO doping and charge-transfer interactions are taking place. FT-IR research confirms the presence of C=C, C-N, and Fe-O vibrations, which in turn confirms the integration of FeO. SEM imaging reveals spherical particles with uneven distribution, while EDAX confirms the presence of C, N, O, and Fe, supporting FeO incorporation.

The wound healing assay on human dermal fibroblast (HDF) cells shows 95-100% wound closure with FPP (50 μ g/ml) within 48 hours, compared to 61% in the control. The rapid closure within 24 hours suggests FPP enhances early-stage wound healing by promoting fibroblast migration and extracellular matrix remodeling. These findings highlight FPP's potential in regenerative medicine and skin repair.

ISSN: 2229-7359 Vol. 11 No. 3S, 2025

https://www.theaspd.com/ijes.php

6. ACKNOWLEDGEMENT

I extend my sincere thanks to Karunya Institute of Technology and Sciences, Coimbatore and Inbiotics Pvt.Ltd, Kanniyakumari.

7. CONFLICT OF INTEREST

The authors declare that there is no conflict of interests regarding the publication of this article.

6. REFERENCES

- 1. Rafique M., Sadaf I., Rafique M. S., and Tahir M. B., A review on green synthesis of silver nanoparticles and their applications, artificial cells, Nanomedicine and Biotechnology. (2016) 45, https://doi.org/10.1080/21691401.2016.1241792, 2-s2.0-85030475399.
- 2. Saif S., Tahir A., and Chen Y., Green synthesis of Iron nanoparticles and their environmental applications and implications, Nanomaterials. (2016) 6, https://doi.org/10.3390/nano6110209, 2-s2.0-84998910214.
- 3. Christian P., der Kammer V., Baalousha F., and Hofmann T., Nanoparticles structure, properties, preparation, and behaviour in environmental media, Ecotoxicology. (2008) 17, 326–343, https://doi.org/10.1007/s10646-008-0213-1, 2-s2.0-44449167276.
- 4 Virkutyte J. and Vara R. S., Chapter 2 environmentally friendly preparation of metal nanoparticles Sustainable Preparation of Metal Nanoparticles: Methods and Applications, 2013, The Royal Society of Chemistry, London, UK, 7–33.
- 5 Bhattacharya D. and Gupta R. K., Nanotechnology and potential of microorganisms, Critical Reviews in Biotechnology. (2005) 25, no. 4, 199–204, https://doi.org/10.1080/07388550500361994, 2-s2.0-28744438873.
- 6. F. Buarki, H. AbuHassan, F. Al Hannan, F. Z. Henari Green Synthesis of FeO Nanoparticles Using Hibiscus rosa sinensis Flowers and Their Antibacterial Activity (2022) https://doi.org/10.1155/2022/5474645
- 7. Das AK, Marwal A and Verma R: Datura inoxia leaf extract mediated one step green synthesis and characterization of magnetite (Fe3O4) nanoparticles. Res Rev J Pharm Anal 2014; 2: 21-24.
- 8. Zhang, Y., Gao, K., Wang, C., & Liu, S. Q. (2021). A novel antibacterial component and the mechanisms of an Amaranthus tricolor leaf ethyl acetate extract against Acidovorax avenae subsp. Citrulli.International Journal of Molecular Sciences, 23(1), 312. http://dx.doi.org/10.3390/ijms23010312. PMid:35008738.
- 9. Rupali Gangopadhyay, Amitabha Be, Conducting Polymer Nanocomposites: A Brief Overview, Chemistry of materials 12 (2000) 608–622.
- 10. https://www.sciencedirect.com/science/article/pii/S0014305799000087
- 11. Yao Tongjie, Lin Quan, Zhang Kai, Zhao Dengfeng, Lv Hui, Zhang Junhu, Yang Bai, Preparation of SiO2 polystyrene@polypyrrole sandwich composites and hollow polypyrrole capsules with movable SiO2 spheres inside, J. Colloid Interface Sci. 315 (2007) 434–438.